Binarisation of Photographed Documents Image Quality and Processing Time Assessment

Rafael Dueire Lins
UFRPE/UFPE, Recife, Brazil
rdl@cin.ufpe.br

Steven J. Simske
Colorado State University, USA
Steve.Simske@colostate.edu

Rodrigo Barros Bernardino
UFPE, Recife, Brazil
rbb4@cin.ufpe.br

ABSTRACT

Smartphones with cameras are omnipresent in today's world and are very often used to photograph documents. Document binarization is a key process in many document processing platforms. This competition on binarizing photographed documents assessed the quality and time performance of 13 new algorithms and 50 existing algorithms. The evaluation dataset is composed of offset, laser, and deskjet printed documents, photographed using four widely-used mobile devices with the strobe flash *on* and *off*, under two different angles and places of capture.

KEYWORDS

Binarization, Documents, Quality evaluation, Time evaluation

ACM Reference Format:

Rafael Dueire Lins, Steven J. Simske, and Rodrigo Barros Bernardino. 2021. Binarisation of Photographed Documents Image Quality and Processing Time Assessment. In *ACM Symposium on Document Engineering 2021 (DocEng '21), August 24-August 27, 2021, Virtual Event, CA, USA.* ACM, New York, NY, USA, 6 pages.

1 INTRODUCTION

According with the report from June 2021 from the consulting firm Strategy Analytics[1], today half of the world's population has a smartphone with a built-in digital camera. The conversion of a color image into its black-and-white version is called *binarization*, or *thresholding*. Such a process is of paramount importance in the pipeline of many document processing systems. No single binarization algorithm is sufficient for all types of text document images [25]. This competition focuses on the binarization of smartphone camera-acquired text documents, the type of document that is most often photographed. This report presents the results of the quality and time performance of 63 algorithms used in the binarization of offset, laser, and deskjet printed text documents photographed at two different places, with four different models of smartphones widely used today, with their in-built strobe flash *on* and *off*.

2 PARTICIPANTS

Eight teams, listed in enrollment order with the affiliation is of their first member, joined this competition:

(A) Harvard University, USA *(Sheng He and L. Schomaker)*: This binarization strategy (**SL**) is based on Tensorflow and the DeepOtsu [13] algorithm. The neural network is trained to learn the degradations in document images and to iteratively produce uniform images. The binarization map is obtained through a global Otsu threshold.

(B) West Pomeranian University of Technology, Poland *(Hubert Michalak and Krzysztof Okarma)*:

MO_1: The input image is downsampled with bilinear and the simple nearest neighbour algorithm, and then it is expanded back to its original size with the same kernel, obtaining the image containing only the low frequency information. Next, this image is subtracted from the original, followed by a simple contrast increase and logical negation and the final image is obtained by applying the Otsu method.

MO_2: The proposed method is based on the equalization of the illumination of an image, increasing also its contrast. Only the relatively high entropy regions should be analysed further as potentially containing some characters, whereas the low entropy regions may be considered as the background. Then, a morphological dilation is performed to increase the contrast, and finally binarization using Bradley's method generates the final image.

MO_3: The image is split into regions and the local thresholds are calculated using $T = a * mean(X) - b$, where $mean(X)$ is the average brightness of the image region and the parameters a and b are subjected to optimization. For each sub-region, the local threshold is determined as the mean of the threshold values calculated for the number of regions dependent on the assumed number of layers and the overlapping factor. Such an approach aims to provide a higher tolerance to rapid illumination changes.

(C) Berlin State Library, Prussian Cult. Heritage Foundation, Germany *(Vahid Rezanezhd, Clemens Neudecker and Konstantin Baierer)*: The solution (**RNB**) is based on machine learning and it is a pixel-wise segmentation model. The dataset used for training is a combination of training sets for binarization competitions in different years with pseudo-labeled images from our dataset in the Berlin State Library. A specific dataset has been produced for very dark or bright images. The model is based on a Resnet50-Unet [32].

(D) AutoHome Corp, Beijing, China *(Huang Xiao, Liu Rong, Xu Chengshen, Li Lin, Ye Mingdeng)*: A combination of binary cross entropy and dice loss is chosen as the loss function of

[1] https://www.strategyanalytics.com/

DocEng '21, August 24–27, 2021, Limerick, Ireland

ACM ISBN 978-1-4503-8596-1/21/08.
https://doi.org/10.1145/3469096.3470833

a deep-learning algorithm. Data augmentation is used in the training process to improve the scores. The original colored or gray images are assigned to equal-size patches, which are fed into either a BCD-Unet [2] ($\mathbf{AH}_1$) or Unet ($\mathbf{AH}_2$) trained models generating binarized patches of dimensions of 128*128 and 256*256, which are then combined back into a large image. Further, a global view with a patch dimension of 512*512 is also used to obtain the final results.

(E) Universitas Syiah Kuala, Indonesia *(Khairun Saddami)*

$\mathbf{KS}_1$: An extension of NICK binarization [37]. The image standard deviation is used to determine the k value which is calculated as $k = -\sigma/(255 - 1.5\sigma)$, where σ is the image standard deviation that represents the image contrast.

$\mathbf{KS}_2$: Combination of Niblack and Wolf [36]. The threshold $T = (2m+mk((\sigma/m)-(\sigma/R)-1))/2$, where σ is the image standard deviation, m is the mean of local window, R is the maximum standard deviation, $k = 0.35$.

$\mathbf{KS}_3$: Combined the local adaptive and global thresholding formulas, as described in [38].

(F) University of São Paulo, Brazil *(Diego Pavan Soler)*: The **DP** method chooses to downscale the input image, rather than using patching, and then rescaling the network output to the input original size. The network architecture used is based on DE-GAN [46], where the input image has been changed to HSV and the hyperparameters and training process have been adjusted, including image augmentation.

(G) University of Fribourg, Sweden *(Jean-Luc Bloechle)*: The **JB** method detects the background using overlapping windows and calculates theirs median color using a quantized color palette. Next, the background image is subtracted from the original image, and the resulting difference image is transformed into grayscale, keeping only the lowest RGB component. A binarization is done by Otsu's algorithm. Detection and removal of small isolated connected components is made. This is a faster and more accurate version of his algorithm in DocEng 2020 Binarization Competition [9].

(H) Hubei University of Technology, China *(Xinrui Wang, Wei Xiong, Min Li, Chuansheng Wang and Laifu Guan)*: The **WX** method comprises three steps: 1) A morphological bottom-hat transform is carried out to enhance the document image contrast, and the size of a disk-shaped structural element is determined by the stroke width transform (SWT). 2) A hybrid pyramid U-Net convolutional network [22] is performed on the enhanced document images for accurate pixel classification. 3) the Otsu algorithm is applied as an image post-processing step to yield the final image.

Fifty previously published binarization algorithms are also part of this assessment: Akbari_1 [1], Akbari_2 [1], Akbari_3 [1], Bataineh [3], Bernsen [5], Bradley [6], Calvo-Z [7], dSLR [42], DilatedUNet [9], DocDLink [53], ElisaTV [44], Ergina_G [45], Ergina_L [19], Gattal [10], Gosh [4], Howe [14], Huali [26], Huang [15], Intermodes [34], ISauvola [12], IsoData [49], Jia-Shi [16], Johannsen [17], KSW [18], Li-Tam [23], Lu-Su [27], Mean [11], Mello-Lins [29], Michalak [9], MinError [21], Moments [48], Niblack [31], Nick [20], Otsu [33], Percentile [8], Pun [35], RenyEntropy [39], Sauvola [40], Shanbhag [41], Singh [43], Su-Lu [47], Triangle [52], WAN [30], Wolf [50], Wu-Lu [28], Yasin [26], Yen-CC [51], YinYang [9], Yuleny [26].

3 TEST SET

Document images acquired using mobile phones are harder to binarize if compared with the use of scanners. The distance between the document and the capturing device and the illumination may vary significantly. Other external light sources and the activation or not of the strobe flash may interfere in the quality of the obtained image. This test set encompasses nine documents obtained from four different models of portable cell-phones (Motorola Moto G9, Apple Iphone SE 2, Samsung Galaxy S20 and Samsung Galaxy A10S), widely used today, whose specifications are presented in Table 1. Besides the device model, the documents in this set were clustered according to having the in-built strobe-flash set as "*on*" or "*off*". The documents in the test set, samples of which are presented in Figure 1, is formed by offset printed book pages, and deskjet and laser printed documents. The whole test set will be included in the DIB dataset (https://dib.cin.ufpe.br) after the publication of the results of this competition.

Table 1: Summary of device camera specifications

	Moto G9	iPhone SE2	Galaxy S20	Galaxy A10S
Megapixels	48	12	64	13
Flash	Dual LED	Quad-LED	Dual LED	Dual LED
Aperture	f/1.8	f/1.8	f/2.0	f1.8
Sensor size	1/2 inch	-	1/1.72 inch	-
Pixel size	0.8 m	-	0.8 μm	-

4 QUALITY-TIME EVALUATION METHODS

Two quality measures were used to evaluate the performance of the binarization algorithms. The first one, P_{err} , compares the proportion between the black-to-white pixels in the scanned and photographed binary documents [25].

The second one made use of Google Vision to perform Optical Character Recognition (OCR) on the documents and applies the Levenshtein distance (L_{dist}) to the correct number of characters in the document transcription ($\#char$). The error rate is calculated as: $[L_{dist}] = (\#char - L_{dist})/\#char$. The measures were ranked in the same way as in [26]. First, the ranking for each measure is calculated for each document in a class. Then, the summation of the rank order for all documents in the class defines the final ranking. Visual inspection was applied to check the consistency of the results obtained.

The processing time evaluation provides the order of magnitude of the time elapsed for binarizing the whole datasets. The training-times for the AI-based algorithms were not computed. The processing device was CPU: Intel(R) Core(TM) i7-10750H CPU @ 2.60GHz, with 32GB RAM and a GPU GeForce GTX 1650 4GB The algorithms were implemented using two operating systems and

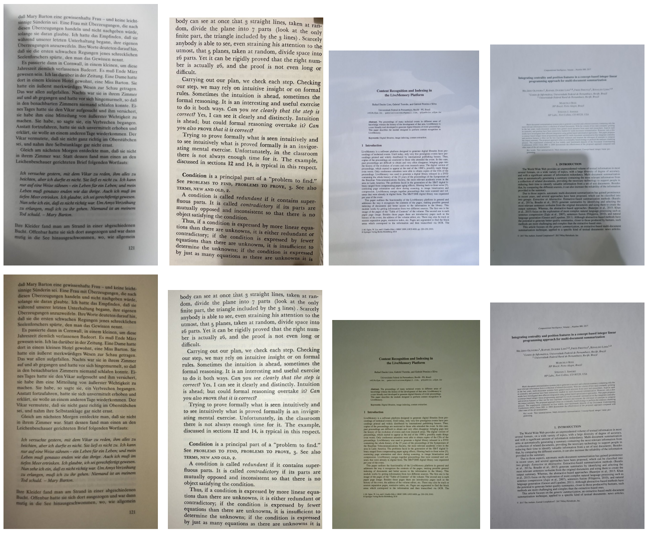

Figure 1: Samples of the images clustered by device (iPhone 6, iPhone SE, Moto Z2, Samsung Galaxy N4) and set-up of the strobe flash (top-line "off", bottom-line "on").

different programming languages, for specific hardware platforms such as GPUs:

- **Windows 10 (version 1909), Matlab:** Michalak21 (team B), Khairun (team E)
- **Linux Pop!_OS 20.10:** DeepOtsu (team A)- Python 2.7 with CPU, Huang BCD and Unet (team D)- Python 3.6 with CPU, DiegoPavan (team F)- Python 3.6, YinYang21 (team G)- Java 14, DilatedUNet (team H)- Python 3.6 with CPU

The algorithms were executed on different operating systems (OS), but on the same hardware. For those that could be executed on both OS types, the processing times for each OS was measured and no significant difference was noticed. This is expected based on a previous edition of this competition [9]. The mean processing time was used in the analysis. The primary purpose is to provide the order of magnitude time of the processing time elapsed. The **SL** algorithm (DeepOtsu) would take weeks to process the images using a CPU; therefore, a NVIDIA Tesla K80 has been used to accelerate the processing. However, an approximation of the CPU processing time is used as reference in order to compare with the other algorithms, each of which was processed using a CPU on the specific platform.

5 RESULTS

The DocEng'2021 Time-quality binarization competition assessed the quality of binary document images produced by 63 algorithms, thirteen new and fifty existing "classic" or more recent ones. The evaluation was performed considering the quality of the produced images and the processing time.

The adopted quality measures were explained above and were used to rank the algorithms. The mean processing time was taken to evaluate the order of magnitude of the time complexity of the algorithms. For all measures, the mean value is presented and the ranking is decided at the individual image level. It is important to remark that the standard deviation of the $[L_{dist}]$ for the Laser and Deskjet dataset was, for nearly all algorithms, approximately 0.04 and for book dataset it was of 0.01, being in some cases close to zero, showing that the top eight algorithms for all test datasets provide exellent binarization results for OCR. This means the results are uniform and, noticeably for the book dataset, the transcriptions are, for the top-8 algorithms, very close the the ground-truth. The standard deviation of the P_{err}, for the book dataset, is close to the mean error, while for Deskjet and Laser dataset, it is, for most cases, between 0.20 and 0.25. This implies in a significant variation in the performance on a per-image basis.

The Huali, Lu-Se, Yuleny, Huang, Johannsen, MinError, Minimum and Intermodes algorithms produced either complete white or black images for some documents, thus they were discarded from the global assessment.

By analyzing the results, several conclusions may be drawn:
1. The new algorithms enrolled in this competition often appear in the top-8 best quality images, showing that the research in this area is yielding better quality algorithms.
2. The ranking order vary among the several configurations of flash and capture device, which reinforce the claim that no binarization algorithm is good for all document images.
3. The quality of the images yielded by the top-8 algorithms with the books pages, offset-printed, dataset are almost perfect if considering the OCR transcriptions precision.
4. Using the same device and capture angle, but turning the strobe flash *on* or *off* had no impact on the P_{err} for the printed (deskjet and laser) datasets, however if using the $[L_{dist}]$, for all cases, the strobe flash state strongly impacts the algorithms ranking. **5.** In some cases, as on the book dataset with Moto G9 or laser dataset with Samsung S20, some old classical algorithms had the best performance. They require a much smaller processing time than the new algorithms, but generated equally good binary images.
6. For many cases, the new algorithms were dominant in the results, as for deskjet dataset with Moto G9. The new algorithms in general are some orders of magnitude slower than the classical ones, and may provide as high quality of images.
7. It is important to remark that the training time of ML algorithms was not considered here.
8. The slowest algorithms are **SL**, DocDLink, **AH**$_1$ and **WX**, which often appear as the best or among the best in a given setup. However, the required processing time does not compensate for the gain in quality for these datasets, as other much faster algorithms presented images of very similar quality.

The recent paper [24], shows that feeding the binarization algorithms with the different RGB channels, instead of the whole image, may yield better quality two-tone image, besides saving processing time. Such a technique will also be considered in future editions of this competition.

ACKNOWLEDGEMENTS

The organisers of this competition are most grateful to all teams enrolled, and to all those who made the code for their algorithms available, for their cooperation and good spirit.

Table 2: Final Results – Dataset of Offset Printed Photographed Book Pages

	Books - Pixel Proportion						**Books - OCR Error**					
	OFF			**ON**			**OFF**			**ON**		
#	**Alg.**	P_{err}	**Time (s)**	**Alg.**	P_{err}	**Time (s)**	**Alg.**	$[L_{dist}]$	**Time (s)**	**Alg.**	$[L_{dist}]$	**Time (s)**
						Motorola G9 Plus						
1	**WX**	0.46	269.34	**MO$_1$**	0.27	0.05	**WAN**	0.99	1.28	**Bradley**	1.00	0.37
2	**MO$_2$**	0.60	3.14	**ElisaTV**	0.37	10.24	**Bradley**	0.99	0.39	**DocDLink**	1.00	275.65
3	**DocDLink**	0.71	286.66	**MO$_3$**	0.40	1.25	**ElisaTV**	0.99	11.03	**Calvo-Z**	0.99	13.24
4	**MO$_3$**	0.58	1.39	**KS$_1$**	0.41	3.39	**ISauvola**	0.99	0.51	**Ergina$_L$**	1.00	0.70
5	**Michalak**	0.60	0.07	**Bradley**	0.66	0.37	**Bataineh**	0.99	0.15	**Michalak**	1.00	0.05
6	**DilatedUNet**	0.94	178.00	**Gattal**	0.68	55.85	**MO$_1$**	1.00	0.06	**IsoData**	0.99	0.18
7	**Bradley**	0.75	0.39	**Michalak**	0.71	0.05	**Akbari$_1$**	0.93	22.06	**AH$_2$**	1.00	87.44
8	**KS$_2$**	0.89	3.65	**Gosh**	0.65	140.94	**KS$_2$**	0.99	3.65	**KS$_2$**	1.00	3.74
						Samsung A10S						
1	**DocDLink**	0.56	173.48	**DocDLink**	0.56	172.01	**Bradley**	0.99	0.24	**SL**	0.99	11627.40
2	**Michalak**	0.55	0.06	**MO$_2$**	0.58	1.91	**RNB**	0.99	28.20	**RNB**	0.99	28.41
3	**MO$_2$**	0.58	2.10	**Michalak**	0.55	0.03	**ISauvola**	0.99	0.33	**Bradley**	0.99	0.23
4	**SL**	0.74	11627.40	**MO$_3$**	0.62	0.78	**SL**	0.98	11627.40	**ISauvola**	0.99	0.33
5	**MO$_3$**	0.62	0.90	**WX**	0.68	174.08	**Bataineh**	0.99	0.09	**AH$_1$**	0.99	260.72
6	**WX**	0.68	174.46	**ISauvola**	0.63	0.33	**MO$_3$**	0.99	0.90	**Bataineh**	0.99	0.09
7	**ISauvola**	0.63	0.33	**KS$_3$**	0.76	4.14	**DocDLink**	0.98	173.48	**MO$_3$**	0.99	0.78
8	**KS$_3$**	0.76	4.17	**Bradley**	0.73	0.23	**MO$_1$**	0.99	0.05	**AH$_2$**	0.99	57.43
						Samsung S20						
1	**WX**	0.36	284.73	**MO$_1$**	0.25	0.04	**DocDLink**	0.99	223.24	**dSLR**	0.99	0.12
2	**DocDLink**	0.37	223.24	**MO$_3$**	0.30	0.93	**RNB**	1.00	35.00	**Bradley**	0.99	0.27
3	**SL**	0.40	10445.59	**Bradley**	0.40	0.27	**Calvo-Z**	0.99	10.99	**SL**	0.99	10088.43
4	**Howe**	0.44	50.20	**Ergina$_L$**	0.41	0.53	**AH$_1$**	1.00	327.99	**DocDLink**	0.99	205.33
5	**Bradley**	0.45	0.30	**Michalak**	0.51	0.04	**SL**	0.99	10445.59	**IsoData**	0.99	0.12
6	**MO$_3$**	0.45	1.13	**IsoData**	0.50	0.12	**MO$_1$**	1.00	0.06	**Li-Tam**	0.99	0.11
7	**DilatedUNet**	0.45	146.80	**Otsu**	0.53	0.02	**Michalak**	1.00	0.06	**ElisaTV**	1.00	6.28
8	**ISauvola**	0.48	0.42	**SL**	0.50	10088.43	**DilatedUNet**	0.99	146.80	**KSW**	0.99	0.12
						Apple iPhone SE 2						
1	**Sauvola**	0.37	0.15	**YinYang**	0.38	1.71	**SL**	0.99	10310.89	**Bataineh**	0.98	0.12
2	**Singh**	0.35	0.23	**JB**	0.39	1.28	**Akbari$_1$**	0.99	20.20	**WX**	0.98	163.15
3	**Gosh**	0.35	78.94	**MO$_1$**	0.40	0.03	**Singh**	0.99	0.23	**Nick**	0.98	0.15
4	**Wolf**	0.48	0.20	**Wolf**	0.38	0.21	**Akbari$_2$**	0.99	20.47	**Singh**	0.98	0.24
5	**YinYang**	0.40	1.74	**Ergina$_L$**	0.47	0.47	**Su-Lu**	0.99	1.67	**Ergina$_L$**	0.98	0.47
6	**KS$_3$**	0.47	4.63	**Ergina$_G$**	0.47	0.35	**Nick**	0.99	0.15	**Bradley**	0.98	0.30
7	**JB**	0.40	1.29	**IsoData**	0.41	0.08	**Akbari$_3$**	0.99	20.40	**KS$_1$**	0.98	3.31
8	**MO$_1$**	0.67	0.08	**KS$_3$**	0.55	4.48	**KS$_1$**	0.99	5.27	**Akbari$_1$**	0.98	20.43

REFERENCES

[1] Y. Akbari *et. al.* 2019. Binarization of Degraded Document Images using Convolutional Neural Networks based on predicted Two-Channel Images. In *ICDAR'19*.

[2] Reza Azad, M. Asadi-Aghbolaghi, M. Fathy, and S. Escalera. 2019. Bi-directional ConvLSTM U-net with densley connected convolutions. *ICCVW 2019* (2019).

[3] Bilal Bataineh, S. N. H. S. Abdullah, and K. Omar. 2011. An adaptive local binarization method for document images based on a novel thresholding method and dynamic windows. *Pattern Recog. Letters* 32, 14 (2011).

[4] Suman K. Bera et al. 2021. A non-parametric binarization method based on ensemble of clustering algorithms. *Multim. Tools and Applications* 80, 5 (2021).

[5] J Bernsen. 1986. Dynamic thresholding of gray-level images. In *ICPR*.

[6] Derek Bradley and G. Roth. 2007. Adaptive Thresholding using the Integral Image. *Journal of Graphics Tools* 12, 2 (2007).

[7] Jorge Calvo-Zaragoza and A. Gallego. 2019. A selectional auto-encoder approach for document image binarization. *Pattern Recog.* 86 (2019).

[8] W. Doyle. 1962. Operations Useful for Similarity-Invariant Pattern Recognition. *J. ACM* 9, 2 (1962), 259–267.

[9] R. Dueire Lins, S. J. Simske, and R. B. Bernardino. 2020. DocEng'20 Time-Quality Competition on Binarizing Photographed Documents. In *DocEng'20*. ACM.

[10] A. Gattal, F. Abbas, and M. R. Laouar. 2018. Automatic Parameter Tuning of K-Means Algorithm for Document Binarization. In *ICSENT*.

[11] C Glasbey. 1993. An Analysis of Histogram-Based Thresholding Algorithms. *Graphical Models and Image Processing* 55, 6 (1993), 532–537.

[12] Zineb Hadjadj et al. 2016. ISauvola: Improved Sauvola's Algorithm for Document Image Binarization. Lecture Notes in CS, Vol. 3212. Springer Berlin Heidelberg.

[13] Sheng He and L. Schomaker. 2019. DeepOtsu: Document Enhancement and Binarization using Iterative Deep Learning. *Pattern Recognition* 91 (2019).

[14] Nicholas R. Howe. 2013. Document binarization with automatic parameter tuning. *International Journal on Document Analysis and Recognition (IJDAR)* 16, 3 (2013).

[15] L. Kai Huang and M. J. J. Wang. 1995. Image thresholding by minimizing the measures of fuzziness. *Pattern Recognition* 28, 1 (1995), 41–51.

[16] Fuxi Jia, C. Shi, K. He, C. Wang, and B. Xiao. 2018. Degraded document image binarization using structural symmetry of strokes. *Pattern Recognition* 74 (2018).

[17] J Johannsen, G and Bille. 1982. A threshold selection method using information measures. In *Int'l Conf. Pattern Recognition*. 140–143.

Table 3: Final Results – Dataset of Deskjet Printed Photographed Documents

	DESKJET - Pixel Proportion						DESKJET - OCR Error					
	OFF			ON			OFF			ON		
	Alg.	P_{err}	**Time (s)**	**Alg.**	P_{err}	**Time (s)**	**Alg.**	$[L_{dist}]$	**Time (s)**	**Alg.**	$[L_{dist}]$	**Time (s)**
#	**Motorola G9 Plus**											
1	**Nick**	0.29	0.23	**Nick**	0.29	0.22	**KS_2**	0.96	3.69	**AH_1**	0.97	420.11
2	**Singh**	0.33	0.52	**Singh**	0.33	0.51	**RNB**	0.95	48.69	**KS_2**	0.96	3.67
3	**Su-Lu**	0.51	2.32	**Su-Lu**	0.51	2.24	**WAN**	0.95	1.48	**SL**	0.97	13666.25
4	**Wolf**	0.51	0.32	**Wolf**	0.51	0.31	**MO_3**	0.96	1.45	**AH_2**	0.96	96.40
5	**KS_1**	0.77	3.46	**KS_1**	0.77	3.46	**$Akbari_1$**	0.95	23.12	**RNB**	0.95	48.68
6	**Yasin**	1.01	1.88	**Yasin**	1.01	1.83	**MO_2**	0.96	3.07	**WAN**	0.95	1.46
7	**Gosh**	1.14	153.41	**Gosh**	1.14	153.41	**Bradley**	0.96	0.44	**MO_3**	0.96	1.45
8	**MO_1**	1.28	0.05	**MO_1**	1.28	0.05	**$Akbari_2$**	0.95	23.08	**MO_2**	0.96	3.08
	Samsung A10S											
1	**Su-Lu**	0.53	1.27	**Su-Lu**	0.53	1.29	**AH_2**	0.97	60.20	**ISauvola**	0.97	0.31
2	**Sauvola**	0.45	0.13	**Sauvola**	0.45	0.13	**ISauvola**	0.97	0.31	**KS_2**	0.97	3.52
3	**Nick**	0.64	0.13	**Nick**	0.64	0.13	**KS_2**	0.97	3.29	**Bradley**	0.97	0.25
4	**Singh**	0.73	0.28	**Singh**	0.73	0.28	**Bradley**	0.97	0.25	**RNB**	0.97	27.67
5	**Yasin**	0.94	1.24	**Yasin**	0.93	1.20	**MO_3**	0.97	0.86	**MO_3**	0.97	0.83
6	**KS_1**	1.02	3.51	**KS_1**	1.02	3.16	**RNB**	0.97	27.61	**JB**	0.97	1.17
7	**Gosh**	1.09	89.11	**Gosh**	1.09	88.44	**JB**	0.97	1.17	**Michalak**	0.97	0.03
8	**Bernsen**	1.13	1.93	**Bernsen**	1.13	1.93	**Michalak**	0.97	0.03	**WAN**	0.97	0.83
	Samsung S20											
1	**Nick**	0.76	0.16	**Wu-Lu**	0.30	0.15	**KS_2**	0.97	3.43	**RNB**	0.97	36.83
2	**Su-Lu**	0.74	1.68	**Su-Lu**	0.96	1.68	**RNB**	0.97	37.60	**dSLR**	0.97	0.15
3	**Singh**	0.82	0.37	**Li-Tam**	1.16	0.15	**WAN**	0.97	1.08	**WAN**	0.97	1.07
4	**Sauvola**	0.99	0.18	**Sauvola**	1.14	0.17	**$Akbari_1$**	0.97	18.68	**RenyEntropy**	0.97	0.15
5	**Wolf**	1.12	0.24	**Gattal**	1.31	55.86	**AH_2**	0.96	74.73	**ISauvola**	0.97	0.40
6	**Gosh**	1.42	117.99	**Nick**	1.33	0.16	**JB**	0.97	1.37	**Moments**	0.97	0.14
7	**Yasin**	1.46	1.69	**Yasin**	1.40	1.63	**$Akbari_2$**	0.97	18.69	**$Ergina_G$**	0.97	0.53
8	**KS_1**	1.08	3.39	**Singh**	1.43	0.36	**$Akbari_3$**	0.97	18.10	**Bradley**	0.97	0.32
	Apple iPhone SE 2											
1	**DP**	0.21	1.59	**Wu-Lu**	0.40	0.17	**YinYang**	0.97	1.68	**RNB**	0.97	36.83
2	**Wu-Lu**	1.07	0.16	**Su-Lu**	0.75	1.94	**$Akbari_1$**	0.97	21.75	**dSLR**	0.97	0.15
3	**Su-Lu**	1.21	1.80	**DP**	0.60	1.61	**Bradley**	0.97	0.36	**WAN**	0.97	1.07
4	**Shanbhag**	0.76	0.16	**Li-Tam**	0.86	0.17	**$Akbari_2$**	0.97	21.93	**RenyEntropy**	0.97	0.15
5	**Yasin**	1.53	1.68	**ElisaTV**	1.03	3.76	**dSLR**	0.97	0.15	**ISauvola**	0.97	0.40
6	**Nick**	1.64	0.18	**Gattal**	1.11	54.10	**$Akbari_3$**	0.97	22.38	**Moments**	0.97	0.14
7	**KS_1**	1.66	3.26	**Yasin**	1.21	1.66	**Otsu**	0.97	0.02	**$Ergina_G$**	0.97	0.53
8	**Singh**	1.74	0.35	**Nick**	1.26	0.19	**Moments**	0.97	0.15	**Bradley**	0.97	0.32

[18] J.N. Kapur et al. 1985. A new method for gray-level picture thresholding using the entropy of the histogram. *Comp. Vision, Graphics, and Im. Proc.* 29, 1 (1985).
[19] E. Kavallieratou and S. Stathis. 2006. Adaptive binarization of historical document images. *ICPR* 3 (2006).
[20] Khurram Khurshid, I. Siddiqi, C. Faure, and N. Vincent. 2009. Comparison of Niblack inspired binarization methods for ancient documents. In *SPIE Proceedings*, Kathrin Berkner and Laurence Likforman-Sulem (Eds.).
[21] J. Kittler and J. Illingworth. 1986. Minimum error thresholding. *Pattern Recognition* 19, 1 (1986), 41–47.
[22] Xiangmao Kong, G. Sun, Q. Wu, J. Liu, and F. Lin. 2018. Hybrid pyramid u-net model for brain tumor segmentation. In *ICIIP*. Springer.
[23] C.H. Li and P.K.S. Tam. 1998. An iterative algorithm for minimum cross entropy thresholding. *Pattern Recognition Letters* 19, 8 (1998).
[24] Rafael Dueire Lins, R. B. Bernardino, et al. 2021. DocEng'2021 Direct Binarization A Quality-and-Time Efficient Binarization Strategy. In *DocEng 2021*. ACM.
[25] Rafael Dueire Lins, R. B. Bernardino, and et.al. 2017. Binarizing Document Images Acquired with Portable Cameras. In *2017 14th ICDAR*. IEEE.
[26] Rafael Dueire Lins, E. Kavallieratou, E. B. Smith, R. B. Bernardino, and D. M. de Jesus. 2019. ICDAR 2019 Time-Quality Binarization Competition. In *2019 15th ICDAR*.
[27] Shijian Lu, Bolan Su, and Chew Lim Tan. 2010. Document image binarization using background estimation and stroke edges. *IJDAR* 13, 4 (2010), 303–314.
[28] Wu Lu, M. Songde, and H. Lu. 1998. An effective entropic thresholding for ultrasonic images. *14th ICPR* (1998).
[29] C A B Mello and Rafael Dueire Lins. 2000. Image segmentation of historical documents. *Visual 2000* (2000).
[30] W. A. Mustafa and A. M. Kader. 2018. Binarization of Document Image Using Optimum Threshold Modification. *J. of Physics: Conference Series* 1019, 1 (2018).
[31] Wayne Niblack. 1985. *An introduction to digital image processing*. Strandberg Publishing Company.
[32] Sofia A. Oliveira, B. Seguin, and F. Kaplan. 2018. dhSegment: A generic deep-learning approach for document segmentation. *CoRR* abs/1804.1 (2018).
[33] Nobuyuki Otsu. 1979. A threshold selection method from gray-level histograms. *IEEE Transactions on Systems, Man, and Cybernetics* 9, 1 (1979).
[34] Judith M. S. Prewitt and M. L. Mendelsohn. 2006. The Analysis of Cell Images. *Annals of the New York Academy of Sciences* 128, 3 (dec 2006), 1035–1053.
[35] T. Pun. 1981. Entropic thresholding, a new approach. *Computer Graphics and Image Processing* 16, 3 (1981), 210–239.

Table 4: Final Results – Dataset of Laser Printed Documents

	LASER - Pixel Proportion						LASER - OCR Error					
	OFF			ON			OFF			ON		
	Alg.	P_{err}	Time (s)	Alg.	P_{err}	Time (s)	Alg.	$[L_{dist}]$	Time (s)	Alg.	$[L_{dist}]$	Time (s)
#	Motorola G9 Plus											
1	Yasin	0.37	1.96	Yasin	0.38	1.85	Akbari$_1$	0.97	22.97	AH$_1$	0.97	406.38
2	Gosh	0.36	142.78	Gosh	0.36	144.64	Akbari$_2$	0.97	22.97	AH$_2$	0.97	92.89
3	Singh	0.45	0.50	Singh	0.45	0.49	Akbari$_3$	0.97	22.94	Akbari$_1$	0.97	22.91
4	MO$_1$	0.48	0.05	MO$_1$	0.48	0.05	MO$_3$	0.97	1.39	Akbari$_2$	0.97	22.96
5	Nick	0.49	0.21	Nick	0.49	0.22	Bataineh	0.94	0.16	Bataineh	0.94	0.16
6	KS$_1$	0.59	3.42	KS$_1$	0.59	3.42	AH$_2$	0.95	96.20	SL	0.96	13666.25
7	Su-Lu	0.42	2.15	Su-Lu	0.42	2.13	Bradley	0.96	0.42	Akbari$_3$	0.97	22.94
8	Bradley	0.71	0.42	Bradley	0.71	0.42	Jia-Shi	0.97	22.97	MO$_3$	0.97	1.40
	Samsung A10S											
1	ElisaTV	0.20	7.27	ElisaTV	0.20	7.31	JB	0.96	1.18	AH$_2$	0.97	56.29
2	Gosh	0.27	80.18	Gosh	0.27	80.18	AH$_1$	0.96	255.79	JB	0.96	1.18
3	Yasin	0.30	1.22	Yasin	0.30	1.27	AH$_2$	0.97	58.18	AH$_1$	0.97	247.14
4	Bernsen	0.33	1.92	Bernsen	0.33	1.91	KS$_2$	0.96	3.25	KS$_2$	0.96	3.29
5	MO$_1$	0.33	0.03	MO$_1$	0.33	0.03	ISauvola	0.96	0.29	Bradley	0.96	0.25
6	Michalak	0.40	0.03	Michalak	0.40	0.03	Bradley	0.96	0.24	ISauvola	0.96	0.29
7	Nick	0.47	0.13	Nick	0.47	0.12	MO$_3$	0.95	0.80	MO$_3$	0.95	0.80
8	Singh	0.47	0.28	Singh	0.47	0.28	RNB	0.97	27.14	RNB	0.97	27.02
	Samsung S20											
1	Gosh	0.15	127.41	Yasin	0.06	1.50	Bradley	0.96	0.33	KSW	0.97	0.14
2	Yasin	0.20	1.68	Sauvola	0.12	0.17	Akbari$_1$	0.89	20.17	RenyEntropy	0.97	0.14
3	MO$_1$	0.40	0.04	Gosh	0.17	105.38	KS$_2$	0.96	3.44	Yen-CC	0.97	0.14
4	Singh	0.49	0.37	IsoData	0.18	0.14	MO$_3$	0.97	1.09	Bradley	0.97	0.31
5	Nick	0.52	0.16	Otsu	0.18	0.02	WAN	0.95	1.09	IsoData	0.97	0.14
6	KS$_1$	0.58	3.40	Gattal	0.19	55.95	Akbari$_2$	0.89	20.18	AH$_2$	0.97	74.26
7	Su-Lu	0.60	1.64	Nick	0.28	0.16	Akbari$_3$	0.89	19.12	Triangle	0.97	0.14
8	Wolf	0.80	0.24	Su-Lu	0.33	1.56	Bataineh	0.96	0.12	KS$_2$	0.97	3.44
	Apple iPhone SE 2											
1	Su-Lu	0.04	1.92	IsoData	0.07	0.16	Bataineh	0.97	0.16	SL	0.97	10310.89
2	Yasin	0.25	1.67	Gosh	0.09	102.36	Sauvola	0.97	0.20	Bradley	0.97	0.37
3	ElisaTV	0.27	5.70	Otsu	0.08	0.02	Bradley	0.97	0.41	Gosh	0.97	102.36
4	DP	0.32	1.66	Nick	0.18	0.19	IsoData	0.97	0.19	YinYang	0.97	1.82
5	Gosh	0.52	99.84	Yasin	0.14	1.57	ISauvola	0.97	0.48	IsoData	0.97	0.16
6	Nick	0.57	0.19	ElisaTV	0.15	3.65	Otsu	0.97	0.02	Wolf	0.97	0.26
7	Sauvola	0.60	0.20	Sauvola	0.21	0.19	Wolf	0.97	0.27	Otsu	0.97	0.02
8	KS$_1$	0.61	3.31	Singh	0.26	0.34	MO$_2$	0.97	2.44	Bataineh	0.96	0.14

[36] Khairun Saddami, P. Afrah, V. Mutiawani, et al. 2018. A New Adaptive Thresholding Technique for Binarizing Ancient Document. In *2018 INAPR*. IEEE.

[37] Khairun Saddami, K. Munadi, et al. 2017. Improved Thresholding Method for Enhancing Jawi Binarization Performance. In *2017 14th ICDAR*, Vol. 1. IEEE.

[38] Khairun Saddami, K. Munadi, Y. Away, et al. 2019. Combination Local and Global Thresholding Method for Binarizing Ancient Jawi Document. *JTIIK* (2019).

[39] Prasanna Sahoo, C. Wilkins, and J. Yeager. 1997. Threshold selection using Renyi's entropy. *Pattern Recognition* 30, 1 (1997).

[40] J. Sauvola and M. Pietikäinen. 2000. Adaptive document image binarization. *Pattern Recognition* 33, 2 (2000).

[41] A.G. G Shanbhag. 1994. Utilization of Information Measure as a Means of Image Thresholding. *CVGIP: Graphical Models and Image Processing* 56, 5 (1994).

[42] J. M. M. Silva, Rafael Dueire Lins, and V. C. Rocha. 2006. Binarizing and Filtering Historical Documents with Back-to-Front Interference. In *ACM SIGAPP 2006*.

[43] T. Romen Singh, S. Roy, O. I. Singh, et al. 2011. A New Local Adaptive Thresholding Technique in Binarization. *IJCSI* 08, 6 (2011).

[44] Elisa B. Smith, L. Likforman-Sulem, and J. Darbon. 2010. Effect of pre-processing on binarization. In *Document Recognition and Retrieval XVII*.

[45] V. Sokratis, E. Kavallieratou, R. Paredes, and K. Sotiropoulos. 2011. A Hybrid Binarization Technique for Document Images. In *Studies in Comp. Intelligence*.

[46] M. A. Souibgui and Y. Kessentini. 2021. DE-GAN: A Conditional Generative Adversarial Network for Document Enhancement. *IEEE T. P. A. M. Int.* (2021).

[47] Bolan Su, S. Lu, and C. L. Tan. 2010. Binarization of historical document images using the local maximum and minimum. In *8th IAPR DAS '10*. ACM Press.

[48] Wen-Hsiang Tsai. 1985. Moment-preserving thresolding: A new approach. *Computer Vision, Graphics, and Image Processing* 29, 3 (1985).

[49] Flavio R. Velasco. 1979. *Thresholding Using the Isodata Clustering Algorithm.* Technical Report. OSD or Non-Service DoD Agency.

[50] Christian Wolf *et. al.* 2003. Text localization, enhancement and binarization in multimedia documents, Vol. 2. IEEE Comput. Soc.

[51] Jui Cheng Yen, F. J. Chang, and S. Chang. 1995. A New Criterion for Automatic Multilevel Thresholding. *IEEE Transactions on Image Processing* 4, 3 (1995).

[52] G W Zack, W E Rogers, and S A Latt. 1977. Automatic measurement of sister chromatid exchange frequency. *Journal of Histochem. and Cytochem.* 25, 7 (1977).

[53] Lichen Zhou et al. 2018. D-linknet: Linknet with pretrained encoder and dilated convolution for high resolution satellite imagery road extraction. In *IEEE CS CCVPR Workshops*.